Risk-Based Seismic Design for Optimal Structural and Nonstructural System Performance

Hugo A. Rojas,[a)] M.EERI, **Christopher Foley,**[b)] M.EERI, **and Shahram Pezeshk,**[c)] M.EERI

An automated performance-based design methodology to optimize structural and nonstructural system performance is outlined and it is shown that it can be used to enhance understanding of structural steel system design for minimum life-cycle costs. Performance is assessed using loss probability with direct economic loss expressed as a percentage of the building replacement cost. Time-based performance assessment is used to compute the expected annual loss of a given steel framing system assuming exposure to three seismic hazard levels. Damage to the structural system, nonstructural displacement-sensitive components, and nonstructural acceleration-sensitive components is characterized using fragility functions. A steel building with three-story, four-bay topology taken from the literature is used to demonstrate application of the algorithm with subsequent comparison of designs obtained using the proposed methodology and others found in the literature. [DOI: 10.1193/1.3609877]

INTRODUCTION

Building codes and design specifications intend to guide the development of structural designs that have acceptable levels of life safety performance when exposed to ground motions, but they provide little direct guidance for altering designs to reduce the potential for damage to the structural and nonstructural systems during a building's service life. The structural engineering profession recognized this limitation and procedures for first-generation performance-based seismic design evolved (ATC 1996, FEMA 2000b). Next generation performance-based engineering (PBE) methodologies are being developed to further address these critical issues and enhance the seismic performance of buildings (FEMA 2000c; FEMA 2006). Several recently completed efforts are assembling the necessary pieces for these next-generation design procedures to be put into practice (FEMA 2007; FEMA 2008).

The common conceptual thread throughout all performance-based engineering methodologies is inclusion of uncertainty. Uncertainty and variability present in predicting seismic demand and response suggest that PBE methods be posed within a risk-based context. A robust conceptual framework for PBE has recently been proposed as the foundation for activities at the Pacific Earthquake Engineering Research (PEER) center. The framework

[a)] CH2M Hill, 9191 S. Jamaica St., Englewood, CO 80112
[b)] Department of Civil and Environmental Engineering, Marquette University, Milwaukee, WI 53233
[c)] Department of Civil Engineering, The University of Memphis, Memphis, TN 38152

Earthquake Spectra, Volume 27, No. 3, pages 857–880, August 2011; © 2011, Earthquake Engineering Research Institute

consists of four main analysis steps (Cornell and Krawinker 2001; Hamburger et al. 2004; Krawinker 2006; Moehle and Deierlein 2004; Zareian and Krawinker 2006a; Zareian and Krawinker 2006b): hazard analysis; structural analysis (ground motion response simulation); damage analysis; and loss analysis. The PEER framework equation is often written in a convenient form to facilitate design-centric (Krawinker 2006; Miranda and Aslani 2003; Moehle and Deierlein 2004) and simplified PBE design and analysis (Zareian and Krawinker 2006a). The mean annual frequency of a decision variable (*DV*) being exceeded can be represented as (Cornell and Krawinker 2001)

$$\lambda(DV) = \int\int\int G(DV|DM)dG(DM|EDP)dG(EDP|IM)d\lambda(IM) \tag{1}$$

where $G(DV|DM)$ is the probability that the *DV* exceeds specified values given that a particular damage measure (*DM*) is reached; $G(DM|EDP)$ is the probability that a *DM* will be exceeded given a particular engineering demand parameter (*EDP*); $G(EDP|IM)$ is the probability that an *EDP* will be exceeded given that a particular intensity measure (*IM*) occurs; and $\lambda(IM)$ is the mean annual frequency (MAF) of an intensity measure (seismic hazard curve). If the most general form of the PEER framework (Hamburger et al. 2004; Krawinker 2006) is to be implemented, probability density functions describing all random variables must be available.

Examples of decision variables are: casualties, direct economic loss, and indirect economic losses. These variables are the basis for goals of minimizing "deaths, dollars, and downtime" resulting from the seismic hazard (Hamburger et al. 2004). Damage measures depend upon the type of building component. Common performance levels that can be associated with the level of damage for structural components are Immediate Occupancy (IO) and Collapse Prevention (CP) (FEMA 2000a; FEMA 2000b). Damage to displacement-sensitive nonstructural building components (NSD), acceleration-sensitive nonstructural building components (NSA), and the structural system (SS) has also been characterized using four damage measures: slight, moderate, extensive and complete (DHS 2003). Typical engineering demand parameters associated with these damage measures include interstory drift, floor acceleration, column compression force, and column splice force.

Decision variables and damage measures can be represented as binary damage state indicator variables (Cornell and Krawinker 2001) and the probabilities, $G(DV|DM)$ and $G(DM|EDP)$, can then be established using fragility curves or fragility surfaces (DHS 2003; FEMA 2006; FEMA 2007). Equation 1 describes a highly complex structural engineering problem because each parameter (*IM*, *EDP*, *DM*, *DV*) remains a continuous random variable. Losses resulting from damage to nonstructural and structural components within the building system are most-often triggered in a discrete manner (Miranda and Aslani 2003). As a result, some of the integrations contained in Equation 1 are often carried out with discrete summation for all pertinent components (Miranda and Aslani 2003). In next-generation PBE methodologies, the decision variables are likely to be conceptualized relatively simply as deaths, dollars and downtime (Hamburger et al. 2004; Hamburger 2004).

There has been a recent trend toward developing formal algorithms for multiple-objective optimal design for seismic hazard where design objectives are to minimize construction cost and attain target performance levels. Many of these previous efforts involved first-generation performance-based design methods (Alimoradi 2004; Alimoradi et al. 2006; Alimoradi et al. 2007; Foley et al. 2007; Liu et al. 2003; Liu et al. 2004a; Liu et al. 2004b; Liu et al. 2005) and some have extended these methodologies to include reliability-based formulations (Tsompanakis and Papadrakakis 2006). There is opportunity to formulate decision-making tools using optimization algorithms (evolutionary computation) and the foundation laid by these next generation seismic design methods.

The present research effort utilizes the PEER framework for performance based engineering within the context of automated and optimized structural design of steel framing systems. The algorithms developed are intended to serve as the foundation for future work in an area of structural engineering design involving decision-making tools that can be used during preliminary and final design phases. Seismic performance is quantified using the probability of direct economic monetary loss expressed as a percentage of the building replacement cost. A risk-based optimization problem is formulated as: (1) minimize the initial capital investment in the structural system; and (2) minimize the expected annual direct economic losses resulting from damage to structural and nonstructural components. An evolutionary algorithm (genetic algorithm, or GA) is used to facilitate automated design of steel frames to meet these multiple performance objectives. Expected annual loss and initial construction cost are incorporated into the GA fitness function along with appropriate penalty formulations to consider constraints. The objectives utilized in the present study focus on average annual direct economic loss as the decision metric.

RISK-BASED DESIGN OPTIMIZATION

Formulating optimization problems involving performance-based engineering concepts begins in the same manner as all optimization problems—with formulation of the objective(s) and constraints. The objectives, however, are slightly more complex because performance is often defined using measures that are quite a bit more involved than traditional optimization problems. It is prudent to provide the reader with a high-level overview of performance-based design so that the present contribution to the body of knowledge can be properly framed. Further details of the design optimization problem and the algorithm used to generate automated and optimized designs will follow the overview.

Figure 1 illustrates a flowchart for the performance-based design methodology implemented in the current research effort within the context of an evolutionary algorithm. The risk-based optimization problem statement used requires complex structural analysis and as a result, an evolutionary algorithm is used to drive the selection of design variables. The present research effort considers planar structural steel framing systems and a reduced search space of design variables taken from the AISC database of steel wide-flange members. Inelastic time history analysis using suites of ground motions characteristic of the seismic hazard selected is used to assess the building performance. The building performance is evaluated using a time-based performance assessment, which is an assessment of probable building performance over a specified period of time, considering all earthquake scenarios that could occur during that period of time, and the probability of occurrence of each. The performance assessment process includes: evaluation of the building's response to earthquake shaking; estimation of damage; consequence of damage incurred (computation of loss). Once the performance assessment is complete, fitness function(s) are computed and

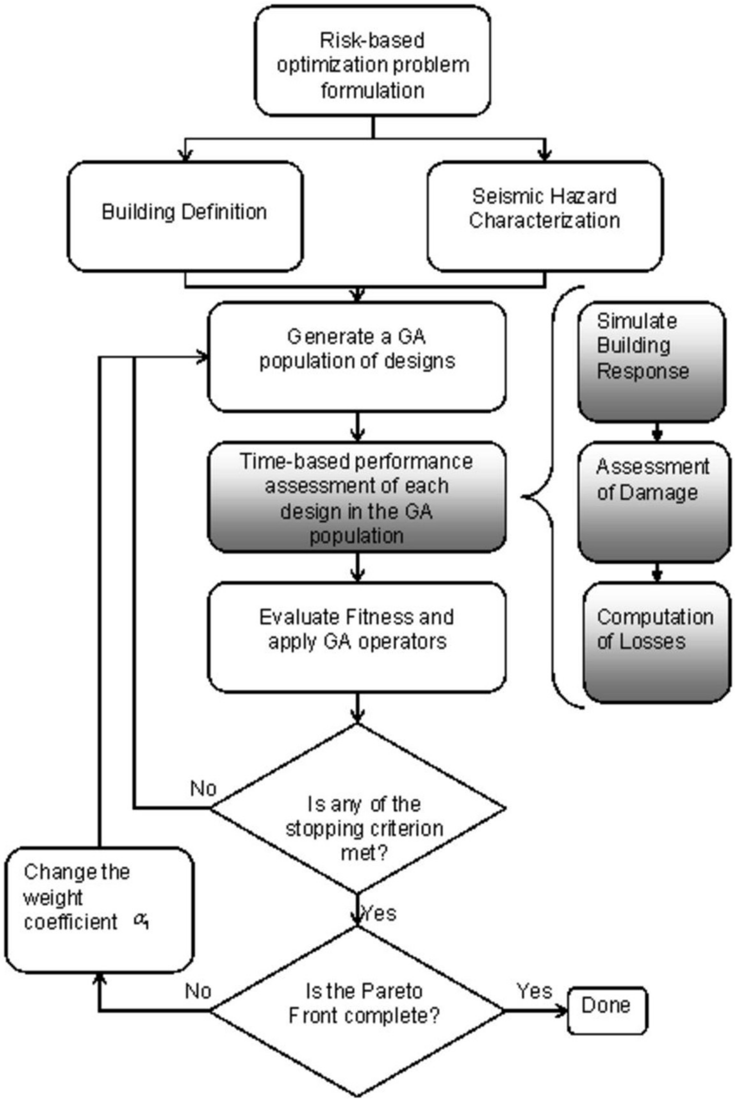

Figure 1. Performance-based design flow chart.

traditional GA reproduction operators are applied to find a new population of candidate designs. The evolutionary procedure is repeated until stopping criteria are met.

RISK-BASED OPTIMIZATION STATEMENT

The first objective of the present research effort is to formulate an optimization problem statement that aligns itself more closely with the needs of all stakeholders in the building process. The second is to develop an algorithm that will provide the structural engineer with decision-making tools to aid in his/her discussions with building stakeholders to enhance understanding of initial capital investment and the resulting impact on exposure to loss. Both of these objectives can be embodied in a risk-based optimization statement and its subsequent solution using evolutionary computation.

When design optimization statements are posed within the common language of all participants in the building process: owners, architects, mechanical/electrical/plumbing engineers, curtain-wall engineers; structural optimization research endeavors can have much greater impact. The present effort considers the following optimization problem statement:

Minimize:
Weight of the Structural System, W
Expected Annual Loss, EAL
Subject To:

$$q^{CP} \geq 0.90 \tag{2}$$

$$q^{IO} \geq 0.50 \tag{3}$$

$$\left(\frac{\sum M_{p,col}}{\sum M_{p,beam}}\right)_i \geq 1.2 \tag{4}$$

where the confidence level in meeting immediate occupancy (IO) performance objective and collapse prevention (CP) performance objective are denoted as q^{IO} and q^{CP}, respectively; $M_{p,col}$, and $M_{p,beam}$ are the plastic moment capacity of a column and a beam, respectively at joint i.

Minimizing the weight is a simplistic way to minimize the initial capital investment in the structural system. It is recognized that fabrication and erection are very important additional metrics for measuring capital investment and past research efforts have incorporated alternate objective formulations to reflect this (Liu et al. 2006). The expected annual loss currently considers direct economic losses resulting from damage to the structural steel system, nonstructural drift-sensitive components, and nonstructural acceleration-sensitive components computed using fragility functions (DHS 2003). Fragility functions (or curves) are mathematical expressions that indicate the conditional probability of incurring damage associated with a particular damage state as a function of a demand parameter.

In this study, HAZUS fragility functions are used to compute probabilities of damage; however, HAZUS fragility curves associated with structural system damage do not provide sufficiently accurate assessment of collapse potential and its ability to be occupied immediately following a ground motion event. As a result, two confidence-level constraints have been included in the optimization problem (FEMA 2000a). Any potential design must have at least 90% confidence in meeting the CP performance objective ($q^{CP} \geq 0.90$) and at least 50% confidence in meeting the IO performance objective ($q^{IO} \geq 0.50$). It is well known that strong-column weak-beam (SCWB) behavior is a desirable characteristic in systems designed to respond to deformations imposed during ground motion events. As a result, the SCWB criteria found in U.S. design specifications (AISC 2005b) for steel systems are included as a third constraint on candidate designs. The present formulation includes uncertainties in engineering demand parameters, intensity measures, and damage measures. There currently is no uncertainty in analysis modeling considered. Further details of the problem formulation are available (Rojas 2008; Rojas et al. 2007).

GA-BASED SOLUTION

The optimization problem statement contains a significant level of complexity in assessing satisfaction of the constraints and the degree to which a design meets the stated objectives for performance. Evolutionary computation has been shown to be very effective at providing candidate design solutions to very complex optimization problems (Foley 2007) and a genetic algorithm (GA) is utilized to tackle the optimization problem formulated in this research.

The GA is an accepted algorithm for engineering optimization and its theory will not be presented here. The interested reader can refer to the seminal work (Goldberg 1989) and other reviews of applications of evolutionary computation in structural engineering research (Foley 2007). The present optimization problem considers two objectives. There are several approaches for handling multiple-objective optimization problems: establishing a single fitness using weighting factors (Alimoradi et al. 2007; Foley et al. 2007); direct utilization of Pareto fronts (Cheng 2002; Cheng and Li 1997); and min-max fitness definitions (Balling and Wilson 2001). Excellent resources describing methods often used in multiple-objective optimization using evolutionary algorithms are available (Deb 2002). In this study, pareto front is used to summarize the optimization results. A pareto front is a plot of the objective functions being optimized where a set of optimum designs that meet all constraints shows a well-defined trend.

The current research effort establishes a single fitness value using weighting factors. The fitness of individual j at generation k during the evolution is assigned using,

$$F_{jk} = \sqrt{\left(\alpha_1 \cdot \left(\frac{W_{\max} - W_{jk}}{W_{\max}}\right)^2 + (1-\alpha_1)\cdot\left(\frac{EAL_{\max} - EAL_{jk}}{EAL_{\max}}\right)^2\right)} \cdot f_{jk}^{CP} \cdot f_{jk}^{IO} \cdot f_{jk}^{SCWB} \quad (5)$$

$W_{\max}$ and $EAL_{\max}$ are the maximum expected values of system weight for the topology considered and maximum expected annual loss for the ground motion records considered, respectively. W_{jk} and EAL_{jk} are the weight and expected annual loss for individual j in generation k of the evolution. α_1 is a weight coefficient that is changed gradually during the evolution from 0 to 1 with 0.05 increment; and f_{jk}^{CP}, f_{jk}^{IO}, and f_{jk}^{SCWB} are penalty functions for ensuring minimum recommended confidence levels in meeting structural performance and for ensuring strong-column weak-beam behavior.

Penalty functions are problem specific and are defined for this study based on methodologies explain in Goldberg (1989) such that convergence is attained as smooth and fast as suitable for the problem. The general form of the penalty functions for immediate occupancy performance, f_{jk}^{IO}, and collapse prevention performance, f_{jk}^{CP}, are given by

$$f_j^Y = \left(2 - \frac{q_j^Y}{q_{\min}^{\mathrm{Y}}}\right)^{-2} \text{ for } q_j^Y \le q_{\min}^{\mathrm{Y}} \quad (6)$$

where Y is the performance objective (collapse prevention, or CP; or immediate occupancy, or IO). $q^Y_{\min}$ is the minimum confidence level in meeting performance Y, and q^Y_{j} is the value of that quantity for individual j. For CP and IO performance-level constraints, these values are set to $q^{CP}_{min} = 0.90$ and $q^{IO}_{min} = 0.50$ as alluded to earlier.

The SCWB requirement is enforced by constraint in Equation 7 which needs to be satisfied at each beam-to-column connection in the structure (i.e., $i = 1, \ldots, N_{jts}$, where N_{jts} is the number of beam-to-column joints). Therefore, penalty function f^{SCWB}_{jk} is evaluated based on the smallest plastic moment capacity ratio over all connections (joints) in the structure, N_{jts},

$$f^{SCWB}_j = \left(2 - \frac{1}{1.2}\left(\frac{\sum M_{p,col}}{\sum M_{p,beam}}\right)_i\right)^{-2} for \left(\frac{\sum M_{p,col}}{\sum M_{p,beam}}\right)_i \leq 1.2 \tag{7}$$

where $M_{p,col}$, and $M_{p,beam}$ are the plastic moment capacity of a column and a beam at joint i, respectively. Further description of the design problem statement and its recasting into an unconstrained (fitness-based) optimization problem suitable for solution using evolutionary computation is available (Rojas 2008).

BUILDING TOPOLOGY

A three-story four-bay frame developed as part of the SAC Joint Venture (FEMA 2000d) is used to illustrate implementation of the algorithm proposed. The topology of the structural steel moment resisting frame considered is shown in Figure 2.

The search space for design of the frame is composed of nine design variables. The structural steel used for all beams and columns in the framework is A992 Grade 50-ksi. The 2-D planar framework analysis model assumes that member centerline-to-centerline dimensions define the topology and no panel zone deformations or rigid end zone modeling is

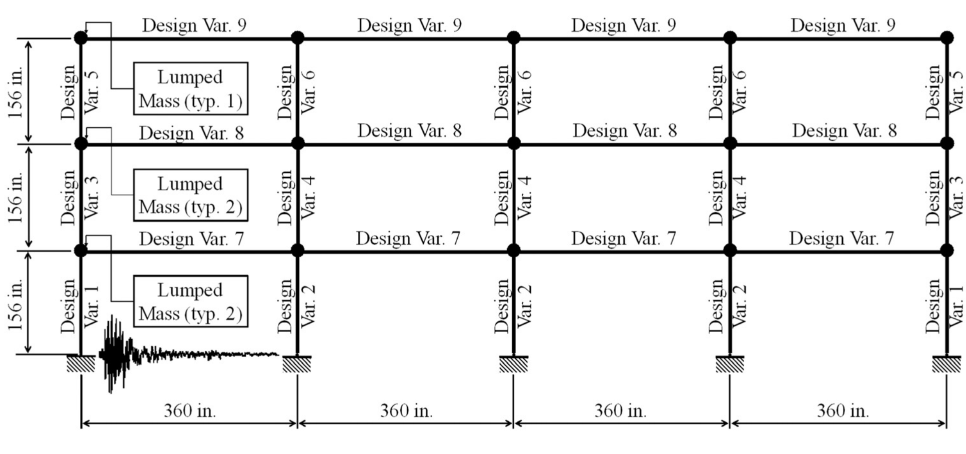

Figure 2. Frame topology for design example.

included. Lumped mass modeling at the beam-to-column connection locations is utilized. The mass of the structure is concentrated at its joints as shown in Figure 2 and its magnitude varies from design to design. No vertical or rotational inertial loads are assumed.

Building components are separated into three different performance groups: structural system components (SS) evaluated using the interstory drift angle (ISDA); nonstructural drift-sensitive components (NSD); and nonstructural acceleration-sensitive components (NSA). The performance of NSD components is quantified using the ISDA, while performance of NSA components is characterized using peak floor acceleration (PFA).

EARTHQUAKE GROUND MOTIONS

Three sets of ten strong ground motion records representing 2%, 10%, and 50% probabilities of exceedence in 50 years (2/50, 10/50, and 50/50, respectively) are selected from the records developed by the SAC steel project (Somerville et al. 1997) for the city of Los Angeles, California. The time histories in this database were scaled. The spectral matching was performed in EZ-FRISK using a time domain approach based on the RSMP99 code of the computer program SpectralMatch developed by Norman Abrahamson (Risk Engineering 2005). The seed ground motions properties and scaling process to obtained the time histories used in this study is presented in detail in (Rojas 2008). The selected and scaled records represent the target design spectra developed according the National Earthquake Hazard Reduction Program (NEHRP) for site category D, firm soil, with de-aggregation of hazards of M6.75-7.5 at closest distance of 2–20 km and M5-7 at 5-15 km for 2/50, 10/50, and 50/50 exceedence probabilities (Somerville et al. 1997). The ground motion acceleration records are used as input for the analytical model to compute the median of peak response quantities (i.e., ISDA, PFA) for the performance-levels associated with the ground motion record probabilities. The thirty horizontal ground motion acceleration records used are shown in Figure 3. No vertical component accelerations are considered.

PERFORMANCE ASSESSMENT

The optimal design problem includes two objectives: weight minimization and minimization of expected annual loss (EAL). A time-based performance assessment of each candidate design is necessary to estimate the EAL and it is the probable earthquake loss considering all potential earthquakes that may occur in a given time period and the mean probability of the occurrence of each. This step in the design process can be subdivided into the following tasks: response simulation; damage assessment; and loss estimation. Inelastic time history analysis (THA) is used to evaluate building response and obtain engineering demand parameter estimates that are used in conjunction with fragility functions to define performance of the SS, NSD, and NSA components under the suites of ground motion accelerations corresponding to each seismic hazard level (2/50, 10/50, and 50/50).

DRAIN-2-DX (Prakash et al. 1993) is used to carry out the inelastic THA required to evaluate the designs during execution of the evolutionary algorithm. A steel beam-column yield surface is used for column members and a beam type surface (no P-M interaction) is used for girders (Powell 1993). The yield surfaces for the beams and beam-columns used are shown in Figure 4.

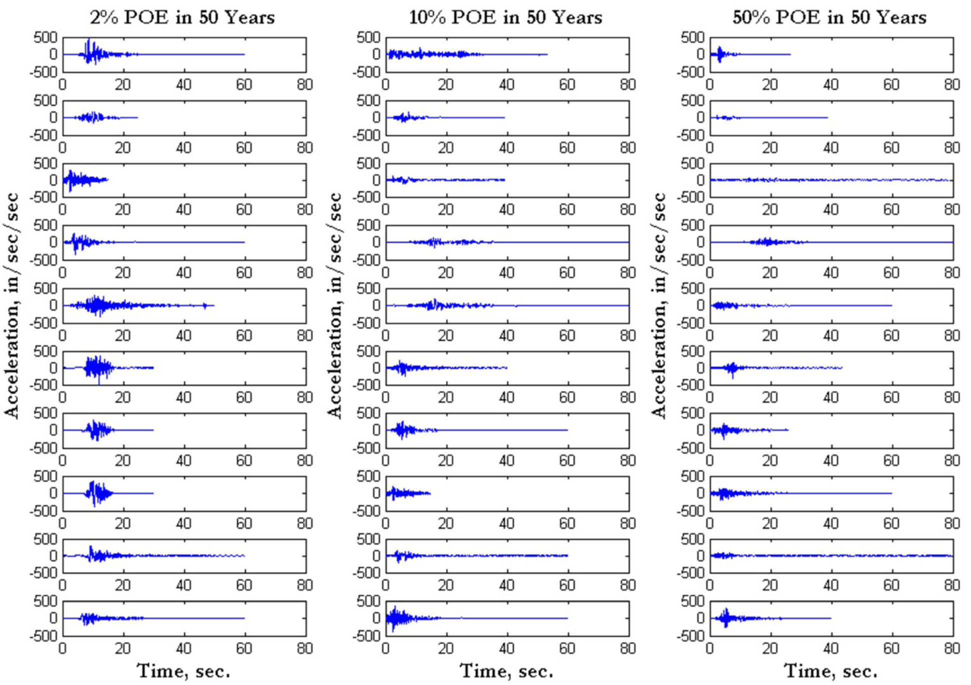

Figure 3. Strong ground motion record sets.

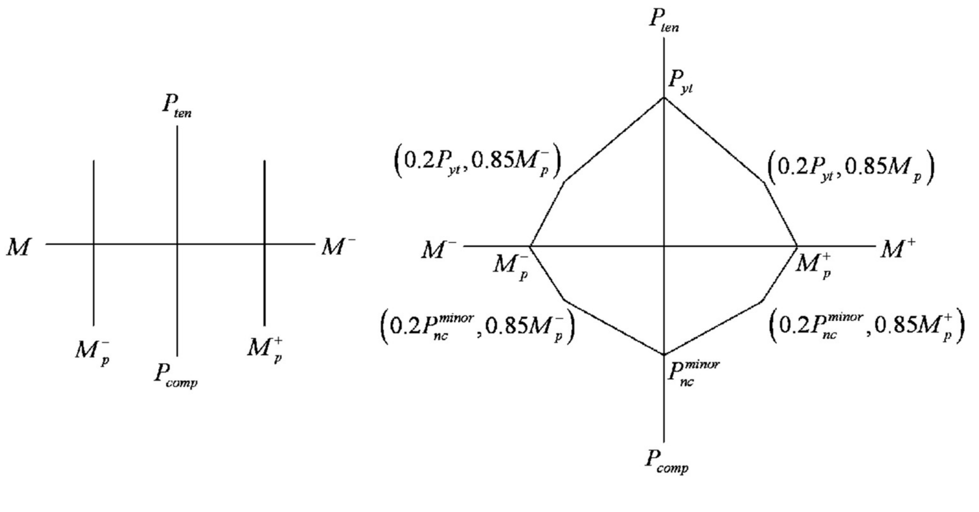

Figure 4. Yield surfaces assumed in the nonlinear response-history analysis: Beam member at the left; and beam-column member on the right.

The axial tensile yield capacity of a beam-column in the absence of bending moment is defined as P_{yt} and it is based upon the yield stress acting on the gross cross-sectional area (AISC 2005a). The axial compression capacity of the beam column in the absence of bending moment is defined as P_{nc}^{minor} and it corresponds to the flexural-buckling capacity of the member about its minor axis of bending assuming that the un-braced length is the story height (156 inches) and the effective length factor is 1.0 (AISC 2005a). M_p^+ and M_p^- are the positive and negative plastic moment capacities of the cross-section about the cross-section's major axis and it is computed assuming no axial loading is present.

The response parameters computed using the inelastic THA are interstory drift angle and peak floor accelerations. Damage to the SS, NSD, and NSA performance groups is characterized using HAZUS fragility functions (DHS 2003) assuming five discrete damage states: none, slight, moderate, extensive, or complete. The conditional probability of a damage measure being at, or exceeding, a particular damage state, *ds*, given any engineering demand parameter, *EDP*, is computed using the normal cumulative distribution function, Φ, given by (DHS 2003)

$$P[DM \geq ds|EDP] = \Phi\left[\frac{1}{\beta_{ds}} \cdot \ln\frac{EDP}{\overline{EDP_{ds}}}\right] \tag{8}$$

$\overline{EDP_{ds}}$ is the median value of the *EDP* considered (e.g., *ISDA*, *PFA*) at which the threshold of a damage state, *ds*, is reached; and β_{ds} is the lognormal standard deviation of the *EDP* and *ds* considered. *ISDA* is used as the engineering demand parameter for characterizing the response of the SS and NSD components. *PFA* is used as the engineering demand parameter characterizing the damage for NSA components. The median values of these parameters (i.e., $\overline{ISDA_{ds}}$ and $\overline{PFA_{ds}}$) as well as the damage-state lognormal standard deviation, β_{ds} used in this study are given in Table 1. These values are similar in magnitude to those used in HAZUS for a High-Code seismic design level based on 1994 UBC lateral force design requirements of Seismic Zone 4) and steel moment resisting frame buildings (DHS 2003).

Computing the probability that the damage measure will be in a specific damage state is done in an indirect manner using the fragility functions. Figure 5 schematically illustrates fragility functions for the 5 damage states considered.

The shaded areas between fragility function curves indicate the damage state probabilities. As an example, consider the EDP (i.e., interstory drift) between the third floor level

Table 1. Fragility curve parameters for structural and nonstructural components

		Damage State			
Component	Curve Parameter	Slight (SLT)	Moderate (MOD)	Extensive (EXT)	Complete (COM)
SS	$\overline{ISDA_{ds}}$	0.004	0.008	0.020	0.0533
	β_{ds}	0.50	0.50	0.50	0.50
NSD	$\overline{ISDA_{ds}}$	0.004	0.008	0.025	0.050
	β_{ds}	0.50	0.50	0.50	0.50
NSA	$\overline{PFA_{ds}}$ (g)	0.30	0.60	1.20	2.40
	β_{ds}	0.60	0.60	0.60	0.60

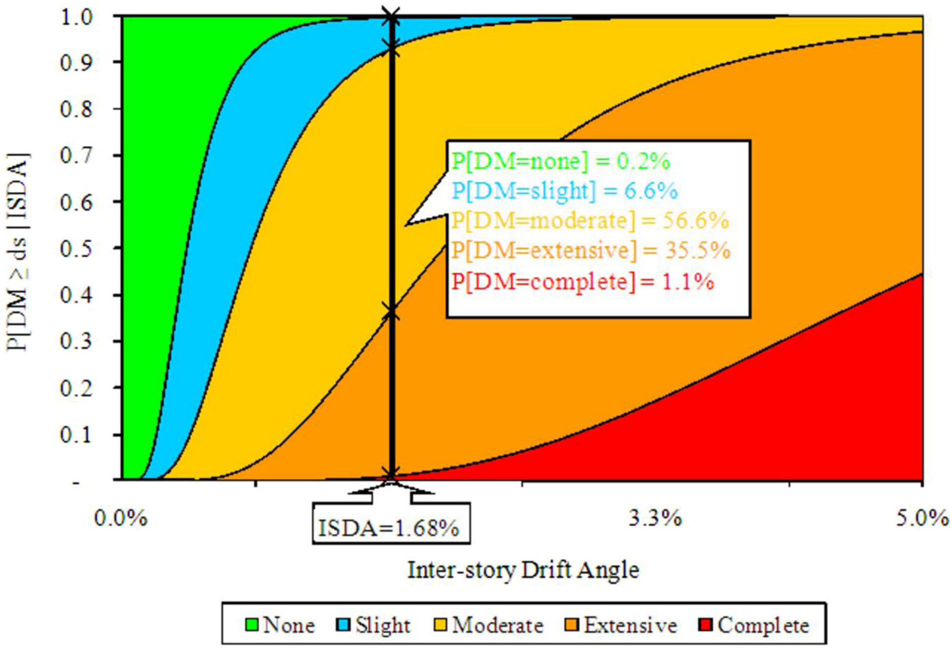

Figure 5. Damage state probability corresponding to engineering demand parameter.

and roof being $ISDA_{3-R} = 1.68$. Given this engineering demand parameter, the probability that the damage will be moderate (MOD) is computed as shown on the figure. Similar computations are performed for structural system (SS), nonstructural displacement-sensitive (NSD), and nonstructural acceleration-sensitive (NSA) components.

Loss estimation resulting from damage to nonstructural and structural components within the building system is based upon direct economic loss (DHS 2003). It is understood that indirect losses (e.g., facility downtime), injuries and deaths are very important considerations. The present formulation can be used to estimate these losses as well as deaths. As a result, it can facilitate the complete "deaths, dollars, and downtime" loss estimate.

The contribution from given component group (e.g., SS, NSD, NSA), to the expected direct economic loss as a percentage of the building replacement cost (BRC) can be estimated using (DHS 2003);

$$E[L^{PG}] = \sum_{ds=2}^{5} P^{PG} \cdot RC_{ds}^{PG} \tag{9}$$

where P^{PG} is the probability of building being in performance group PG damage state ds. RC_{ds}^{PG} is the repair cost ratio for performance group PG due to damage state ds. The damage measure, ds, varies from slight (SLT, 2) to complete (COM, 5). The damage state of none

Table 2. Repair cost ratios (RC_{ds}^{PG}) expressed as percentage of building replacement cost (DHS 2003)

	Damage State			
Performance Group: *PG*	Slight (SLT)	Moderate (MOD)	Extensive (EXT)	Complete (COM)
SS	0.4	1.9	9.6	19.2
NSD	0.7	3.3	16.4	32.9
NSA	0.9	4.8	14.4	47.9
Total	2.0	10.0	40.4	100.0

(NON) does not contribute to the loss summation. The repair cost ratios expressed as a function of the building replacement cost (BRC) used in this study are given in Table 2.

The total expected direct loss is the summation of the expected loss for all performance groups considered (i.e., SS, NSD, and NSA),

$$E[L_T|IM] = E[L^{SS}|IM] + E[L^{NSD}|IM] + E[L^{NSA}|IM] \tag{10}$$

For any given ground motion, the performance groups will have expected probabilities of being in specific damage states given an engineering demand parameter. For the three-story topology, there are three potential interstory drifts and three potential peak floor accelerations from which to evaluate damage. Rather than computing expected loss at each floor level or story, the mean interstory drift and mean peak floor acceleration are used as the basis of loss computations. As a schematic example, probabilities of being in NON, SLT, MOD, EXT, COM damage states are determined to be 0.17%, 5.93%, 54.63%, 37.93%, and 1.33%, respectively. These mean probabilities must all sum to 100% and the damage state probabilities can be expressed in bar-graph fashion as shown in Figure 6. The probability of extensive damage given a mean ISDA is explicitly indicated on the bar graph.

The bar graphs shown in Figure 6 also illustrate the distribution of damage states for the SS, NSD and NSA components. The schematic example given in Figure 6 illustrates the total expected direct economic loss for SS, NSD and NSA components would be 18.19% of the building replacement cost.

The simple example in Figure 6 illustrates computation of the expected loss for one ground motion and one realization of the mean engineering demand parameters. The process schematically depicted in Figure 6 is repeated for each ground motion in the suite of ground motions to obtain a cumulative distribution of losses for each hazard level: 50/50, 10/50, and 2/50. Total repair costs (expected direct economic loss) for all ground motions at all hazard levels are computed and these repair costs are used to fit a lognormal cumulative distribution function (CDF) describing the probability of total repair cost exceeding a defined value. Therefore, a continuous range of probabilities can be used in lieu of the discrete values taken from the ten ground motion simulations. Sample CDFs as well as more detail explanation of the process is available in (Rojas 2008).

Time-based performance assessment is an estimate of the probable earthquake loss considering all potential earthquakes that may occur in a given time period and the mean

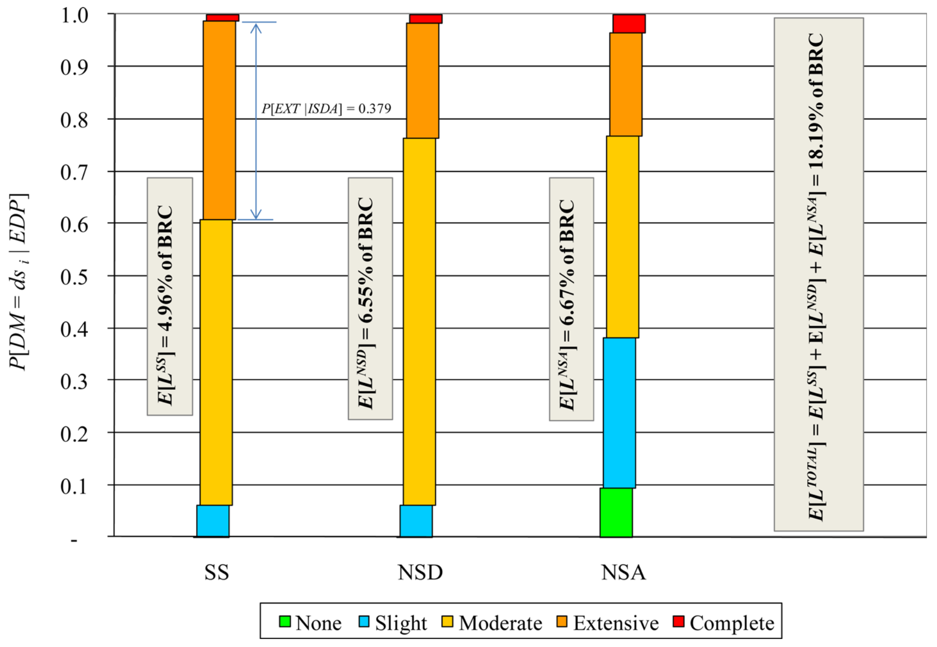

Figure 6. Loss analysis for example distribution of losses.

probability of the occurrence of each. The earthquake-intensity variable is described by a seismic hazard curve, which plots the relationship between earthquake intensity and its mean annual frequency of exceedence. The hazard curve considered in the present study is given in Figure 7. Expected Annual Loss (EAL) curves are developed for intensities of earthquake shaking that span the intensity range of interest and are then integrated (summed) over the hazard curve using

$$P[RC_T > rc_T] = \int_{\lambda} P[RC_T > rc_T|IM]d\lambda(IM) \approx \sum_{i=1}^{3} (1 - P[RC_T \leq rc_T|IM_i]) \cdot \Delta\lambda(IM_i) \tag{11}$$

where $(1 - P[RC_T \leq rc_T|IM_i])$ is the probability of loss exceeding rc_T for an earthquake with intensity of IM; $\Delta\lambda(IM_i)$ is the mean annual recurrence interval of a given ground motion intensity; and i is the hazard level.

There are three hazard levels over which the losses are aggregated. As a result, Equation 11 can be written as

$$\begin{aligned} P[RC_T > rc_T] = & \left(1 - P\left[RC_T \leq rc_T|IM_{2/50}\right]\right) \cdot \Delta\lambda\left(IM_{2/50}\right) \\ & + \left(1 - P\left[RC_T \leq rc_T|IM_{10/50}\right]\right) \cdot \Delta\lambda\left(IM_{10/50}\right) \\ & + \left(1 - P\left[RC_T \leq rc_T|IM_{50/50}\right]\right) \cdot \Delta\lambda\left(IM_{50/50}\right) \end{aligned} \tag{12}$$

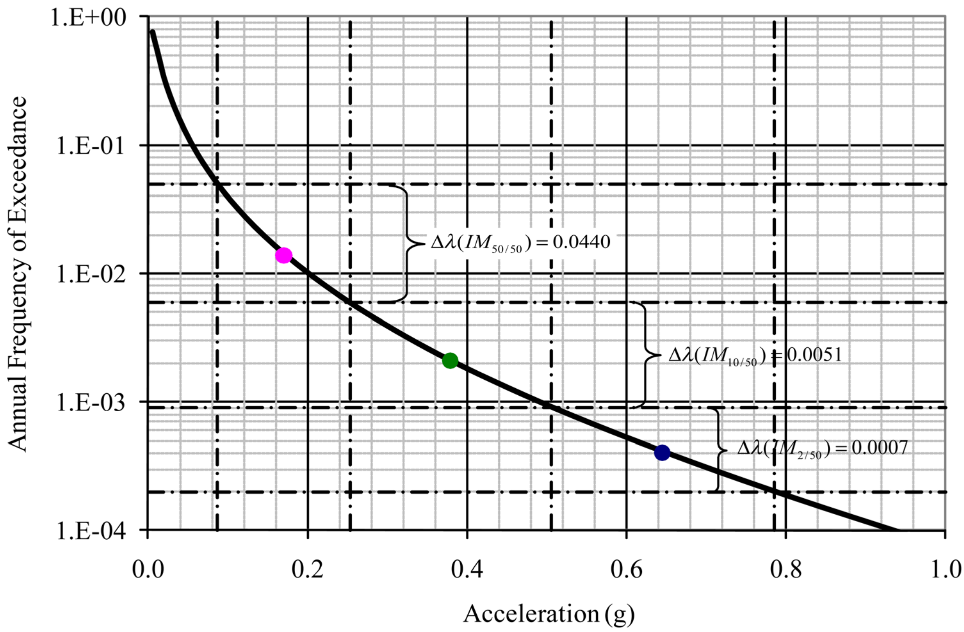

Figure 7. Peak ground acceleration hazard curve used in the present study.

$P[RC_T \leq rc_T|IM_i]$ is obtained from the lognormal cumulative distribution function fitted to the data from each ground motion and $\Delta\lambda(IM_i)$ are obtained from the hazard curve. The range of mean spectral acceleration of interest was selected as 0.08 g to 0.79 g; the lower limit was selected to avoid getting into the most variable part of the hazard curve and the upper limit is the spectral acceleration corresponding to a mean annual frequency of exceedance of 0.0002. This range of mean spectral acceleration was split into three intervals so that the midpoint value in each interval matches the probability of exceedance that characterizes each set of time histories used in the study. Figure 7 shows a hazard curve for Los Angeles (city considered in this study) split into three discrete intervals resulting in the following mean annual recurrence interval: $\Delta\lambda(IM_{50/50}) = 0.0440$; $\Delta\lambda(IM_{10/50}) = 0.0051$; and $\Delta\lambda(IM_{2/50}) = 0.0007$.

Aggregated loss from all intensity measures is obtained by multiplying each lognormal CDF fit to the ground motion loss data by the annual frequency of shaking in the interval of earthquake intensity used to construct the loss curve. A summation of the annual frequencies for a given value of the loss is therefore given by Equation 12.

A higher-level description of loss can be termed the expected annual loss. Annualized loss is a powerful metric for those tasked with defining standards of performance for a building. The mean expected annual total loss (EAL) is computed by integrating the aggregated loss curve (Figure 8). The example shown in this figure illustrates an expected annual loss of approximately 0.653% of the building replacement cost. The expected annual loss is

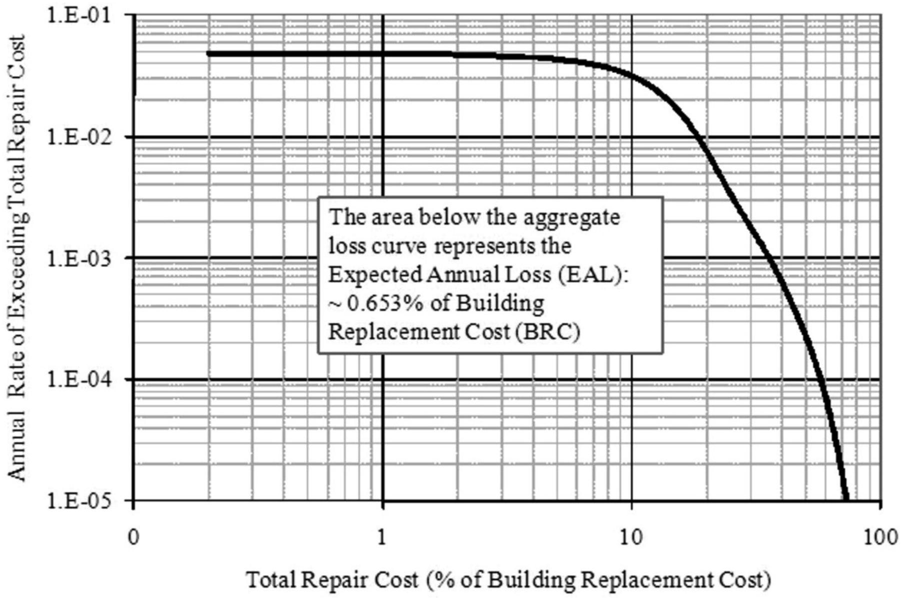

Figure 8. Example aggregated (annual) loss.

one of the objectives used in the present design optimization and the previous discussion illustrates the layers of complex structural analysis required to evaluate this objective. As a result, the optimization problem considered in this study is extremely complicated and mathematical (gradient-based) optimization procedures simply cannot be formulated to guide member selection for the frame topology chosen.

GENETIC ALGORITHM

The complexity of the optimization problem tackled in this study precludes application of mathematical (gradient-based) optimization algorithms. Evolutionary algorithm-based procedures have been shown to be very powerful tools to solve widely varying and complex optimization problems (Foley 2007) and a genetic algorithm is employed in this study to guide member selection and facilitate automated design of the framing systems and generation of decision tools. The fundamental theory and application of the genetic algorithms is very well defined and details will not be provided here. The interested reader can find typical formulations of genetic algorithms in several textbooks (Coley 2001; Deb 2002; Goldberg 1989) and a review of application and fundamental theory is available (Foley 2007).

The expected annual loss and system weight are used to establish candidate fitness according to Equation 5. After evaluating the performance of each design in the GA population, GA reproduction operators (i.e., crossover, mutation) are applied to find a new population. This procedure is repeated until there is no increase in the fitness of the most highly fit individual over the previous 20 generations, or a maximum number of generations equal to 300 is reached.

An existing genetic algorithm driver (Carroll 2004) is used in the present study because of its reliability and the ability to tune the genetic algorithm using a wide variety of well documented mechanisms. Application of the genetic algorithm in this study includes a population size of 100, probability of crossover of 60%, and probability of mutation of 3.5%. Reproduction includes parent chromosomes producing two offspring with 4.0% probability of creep (Carroll 2004). It should be noted that intelligent GA operators (e.g., mutation, crossover) similar to the adaptive strategies to be used in this work have been utilized to tackle very complex optimization problems (Foley and Schinler 2001; Foley and Schinler 2003; Foley et al. 2002; Schinler and Foley 2001; Voss and Foley 1999a; Voss and Foley 1999b) and have been shown to be robust tools to solve very complicated optimization problems. Such operators are not used in the present study.

The search space for the GA is composed of 64 AISC steel wide-flange sections with compact cross-section typically used for columns (e.g., W14, W12, W10, and W8) and 64 AISC steel wide-flange sections with compact cross-section typically used for beams (e.g., W44, W40, W36, W33, W30, W27, W24, W21, W18, W16).

The computational cost of the implemented formulation depends on the number of degrees of freedom of the structure; the complexities of the objective function and search space; the number, duration, and sampling rate of the strong ground motion input records; and the level of gravitational forces on the frame. To complete one design, the GA runs with a population of 100 chromosomes in 300 generations under 30 ground motions which require 900,000 inelastic second-order dynamic analysis. Although the amount of computations performed is expensive none of the cases studied in this research required more than 48 hours of computer run time.

RESULTS AND DISCUSSION

Twenty-one GA runs were performed while changing the weighting coefficients found in Equation 5. The values of α_1 varied from 0 to 1 with an interval equal to 0.05. These 21 runs generated many candidate designs. All potential designs generated are compiled and presented in Figure 9. The scatter plots of designs shown in this figure illustrate decision space for the risk-based design problem. Each marker in the cloud of markers is a potential design for the three-story, four-bay frame topology. The size and color of each marker represents scaling according to: fitness, penalty for CP performance, penalty for IO performance, and penalty for SCWB criteria.

The scaling and coloring allows active constraint regions to be identified. The red areas represent the feasible region for the optimization problem since all constraints are satisfied for those designs are indicated by their scaling magnitudes being 1.0. A Pareto set of solutions can be identified in the upper left graph. The markers along the feasible Pareto set of all solutions are scaled to larger size on this front and their color is darkest. These candidate solutions will be used in later discussion as they comprise a decision making tool for the structural engineer. Upon examination of graph in the upper right, it can be seen that structural systems weighing more than approximately 52 kips and having EAL magnitudes equal

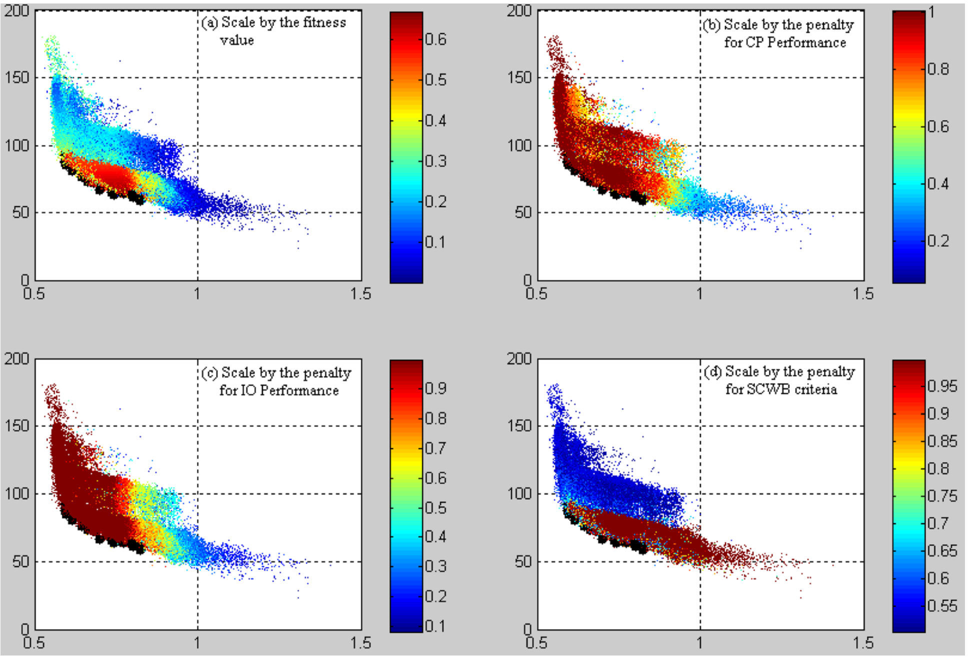

Figure 9. Decision space and feasible region for designs generated.

to or less than approximately 0.75% of the building replacement cost will satisfy the constraints for collapse prevention (CP) performance. A similar statement can be made after examining the IO performance constraint scaling in the lower left. The lower right graph indicates a candidate design with weight exceeding 75 kips will not satisfy the strong column weak beam constraint. The twelve feasible designs found on the Pareto front shown in the upper left graph of Figure 9 are plotted in decision space in Figure 10.

A trend-line is shown on the figure and this line outlines (schematically) a continuous Pareto front defined by the designs generated by the GA. As expected, a heavier structure results in lower expected annual loss as a function of the building replacement cost. Lighter structural systems (conceivably less costly to construct) experience higher expected annual loss. This behavior is to be expected and the GA-based decision tool appears to be capable of capturing expected behavior for the present optimization problem.

A very powerful way of using Figure 10 is to define additional costs, annual benefits, and a return on investment that can be used as a means of deciding between alternatives. The rate of return (ROI) is a simple expression of the equivalent interest rate that would be obtained from a particular investment. For a long duration investment, such as 50 years, the return on investment can be calculated as the annualized benefit of the investment divided by the cost of the investment. This is the goal of performance-based engineering and the algorithm presented is clearly capable of providing the decision-making tools needed to have all stakeholders in a given project speaking a common language.

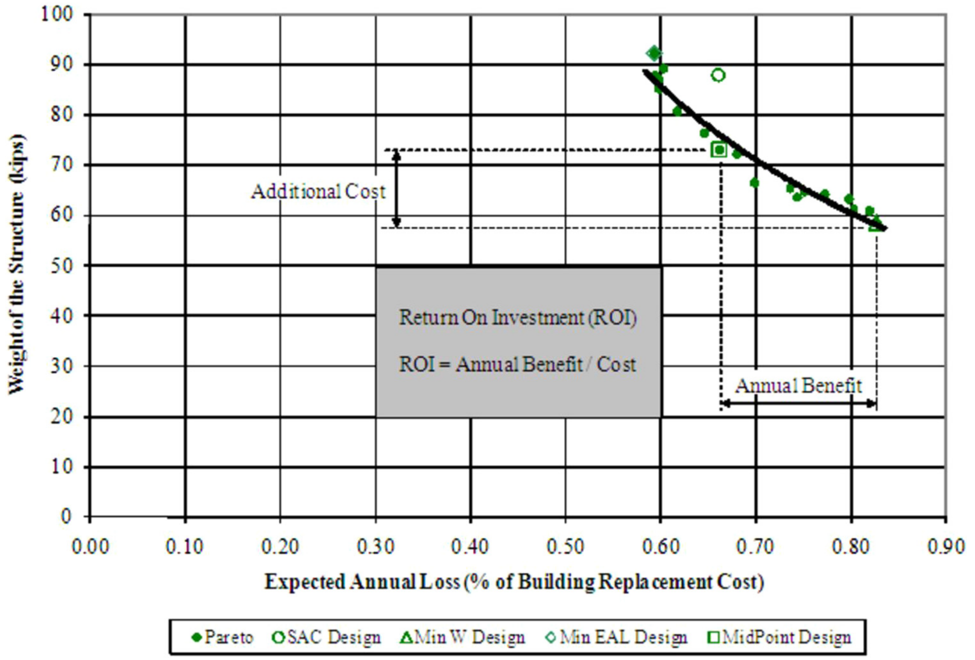

Figure 10. Pareto front for frame designs generated and return on investment definition.

As demonstration of how the results of the present GA runs can be used in the decision-making process, a comparison between four alternative designs will be made. The designs to be compared are: the design with minimum expected annual loss; the design with minimum weight (initial construction cost or investment); the design at the midpoint in the Pareto front; and the SAC building design (FEMA 2000d; FEMA 2000e) shown as the hollow circle. These designs are identified in Figure 10. Table 3 shows the steel wide-flange sections selected by the current GA implementation and those used in the SAC project (FEMA 2000d; FEMA 2000e).

Table 4 contains performance information for these four designs for the thirty ground motions considered, and Figure 11 presents this data in graphical form. The information contained in Table 4 and Figure 10 indicates that the Pareto front identified by the current GA implementation contained designs that spanned that used in the SAC research effort. This is very encouraging as the present formulation contained different design objectives than this former effort, yet the framework used in the SAC study has performance characteristics very similar to those of the GA-based designs generated in this study.

The present algorithm was able to generate a mid-point design that was significantly lighter than the SAC design with comparable expected annual loss. CP and IO structural system performance objectives had similar confidence levels with the SAC design having higher confidence for CP performance and lower confidence for IO performance. When the minimum weight GA design is considered, the expected annual loss rises significantly and

Table 3. Pareto front designs generated via current algorithm and sizes reported in SAC research effort (FEMA 2000d; FEMA 2000e)

Design	Story	Columns: Exterior	Columns: Interior	Girder
SAC	1	W14x257	W14x311	W30x116
	2	W14x257	W14x311	W30x116
	3	W14x257	W14x311	W24x62
Min W GA	1	W14x311	W14x311	W24x76
	2	W14x176	W14x233	W30x90
	3	W14x68	W14x193	W18x40
Midpoint GA	1	W14x257	W14x311	W27x84
	2	W14x159	W14x283	W30x108
	3	W14x99	W14x257	W24x55
Min EAL GA	1	W14x283	W14x311	W30x90
	2	W12x336	W12x336	W33x118
	3	W12x279	W12x336	W27x84

the IO performance confidence level for the structural system becomes very close to the limit (50%). The confidence level for CP structural performance remains high (92%).

The distribution of loss data in Figure 11 shows the proportion of total expected annual loss that is attributed to nonstructural system components. NSA component loss tends to become a larger percentage of the total expected annual loss as the hazard level decreases. It is very interesting to note that the minimum weight GA design is a flexible system and the

Table 4. Performance information for three-story, three-bay frame designs

						Distribution of Losses			
Design	Hazard Level	W kips	EAL (% BRC, or %)	q^{CP} (% BRC, or %)	q^{IO} (% BRC, or %)	Median RC (% of BRC)	SS (% of Median RC)	NSD (% of Median RC)	NSA (% of Median RC)
SAC	2/50	88.00	0.653	98.15	85.84	42.10	25.72	42.32	31.96
	10/50					21.91	24.29	34.35	41.36
	50/50					11.59	20.25	27.89	51.86
Min W	2/50	58.60	0.826	91.97	52.99	49.17	28.07	47.97	23.96
	10/50					22.61	28.59	41.22	30.20
	50/50					15.12	24.38	34.98	40.65
Mid-Pt	2/50	73.18	0.662	90.38	93.56	42.72	26.39	43.58	30.04
	10/50					19.93	26.18	36.34	37.48
	50/50					11.78	20.96	30.14	48.90
Min EAL	2/50	92.35	0.593	96.44	95.67	36.24	24.30	39.64	36.06
	10/50					16.97	21.88	30.67	47.45
	50/50					10.80	16.69	24.44	58.87

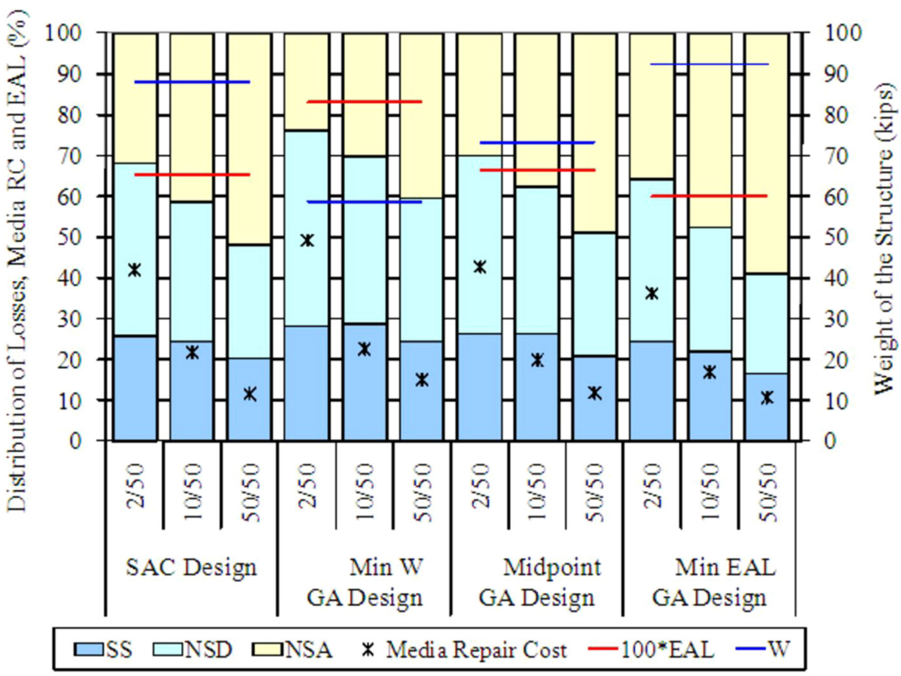

Figure 11. Graphical depiction of loss distribution.

percentage of EAL coming from NSA component damage is the smallest for all three hazard levels. The structural framing system is likely acting to isolate ground motion acceleration from the floor levels. As expected, the NSD component contribution to the total expected annual loss is among the largest for all designs at all hazard levels.

The median repair cost for all designs at each hazard level in Table 4 illustrates that as the hazard level decreases, the median repair cost decreases. The reduction is most significant for the minimum weight design on the Pareto front. The minimum EAL design, the mid-point design, and the SAC design all illustrate very similar trends with very similar magnitudes in reduction with hazard level increase.

Figure 12 presents the aggregated loss function for the designs in Table 3. This figure can be used to evaluate the expected annual repair cost for any annual frequency of exceeding a defined repair cost in a manner similar to that of a seismic hazard curve. In other words, one can enter Figure 12 with a target total repair cost (e.g., 15%) and read off an expected annual rate of exceeding this total repair cost (e.g., ∼0.002 or ∼0.2% for the min. EAL design). Thus, the GA-generated designs can be used to gain a fairly detailed picture of building loss magnitudes and the expected annual rates of exceeding these losses.

CONCLUDING REMARKS

The algorithms and tools developed through this research can help the structural engineering profession implement PBE in a consistent, understandable, and repeatable manner

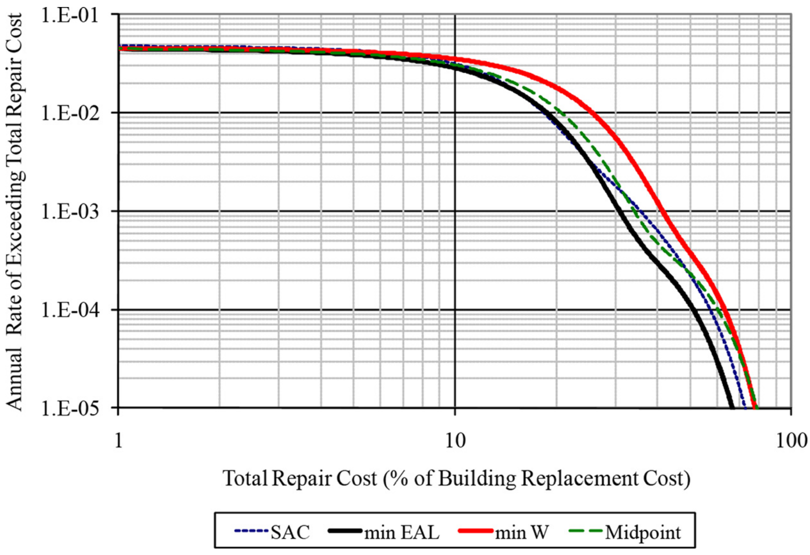

Figure 12. Aggregated loss function for designs generated in present study.

in the design process of steel frames. These tools help the structural engineering profession provide all stakeholders in a building project with decision-making tools suitable for risk-based structural engineering design for seismic hazard and mechanisms to evaluate alternative designs. These algorithms and methods also allow the structural engineering profession to easily compare and contrast the structural designs with regard to expected performance.

The present study developed a methodology for quantifying the impact that initial capital investment has on minimizing expected annual loss. The method outlined also illustrated how the total repair cost can be de-aggregated to identify which component contributes the most to the total repair cost, providing useful information in making design decisions. The results also illustrated tradeoffs that will likely arise when stiff and flexible building systems are considered.

The automated design algorithm presented was able to generate a Pareto front that facilitates decision making processes. Using the return on investment, the benefits and costs of moving along the Pareto front from one alternative design to another could be compared on a sound and consistent economic basis.

REFERENCES

American Institute of Steel Construction (AISC), 2005a. *Load and Resistance Factor Design Specifications for Structural Steel Buildings*, American Institute of Steel Construction, Chicago, IL.

American Institute of Steel Construction (AISC), 2005b. *Seismic Provisions for Structural Steel Buildings Including Supplement Number 1 (ANSI/ASCE 341s-05)*, American Institute of Steel Construction, Chicago, IL.

Alimoradi, A., 2004. Probabilistic Performance-Based Seismic Design Automation of Nonlinear Steel Structures, Ph.D. Thesis, The University of Memphis.

Alimoradi, A., Pezeshk, S., and Foley, C. M., 2006. Evolutionary seismic design for optimal performance, in *Intelligent Computational Paradigms in Earthquake Engineering*, N. D. Lagaros and Y. Tsompanakis, eds., Idea Group Publishing, Hershey, PA, 42–58.

Alimoradi, A., Pezeshk, S., and Foley, C. M. 2007. Probabilistic performance-based optimal design of steel moment resisting frames: Part 2 – applications, *Journal of Structural Engineering* **133**, 767–776.

Applied Technology Council (ATC), 1996. *ATC - 40: Seismic Evaluation and Retrofit of Concrete Buildings - Volume 1, Report No. SSC 96-01*, Applied Technology Council, Redwood City, CA.

Balling, R. J., and Wilson, S. 2001. The maxi-min fitness function for multi-objective evolutionary computation: Application to city planning, *Genetic and Evolutionary Computation Conference (GECCO 2001)*, San Francisco, CA, Morgan Kaufmann, 1079–1084.

Carroll, D. L. 2004. *FORTRAN Genetic Algorithm Driver*, CU Aerospace (http://cuaerospace.com/carroll/ga.html), Champaign, IL.

Cheng, F. Y., 2002. Multiobjective optimum design of seismic-resistant structures, *Recent Advances in Optimal Structural Design*, S. A. Burns, ed., American Society of Civil Engineers, Reston, VA, 241–256.

Cheng, F. Y., and Li, D. 1997. Multiobjective optimization design with pareto genetic algorithm, *Journal of Structural Engineering* **123**, 1252–1261.

Coley, D. A., 2001. *An Introduction to Genetic Algorithms for Scientists and Engineers*, World Scientific Publishing Co., Pte., Ltd., Singapore.

Cornell, C. A., and Krawinker, H., 2001. A framework for performance-based design 2001: A structural engineering Oodyssey, in *Proceedings of the 2001 Structures Congress and Exposition*, American Society of Civil Engineers, Reston, VA, CD-ROM.

Deb, K. 2002. *Multi-Objective Optimization Using Evolutionary Algorithms*, John Wiley & Sons, Ltd., Chichester, UK.

Department of Homeland Security (DHS), 2003. *HAZUS-MH MR1: Advanced Engineering Building Module, Technical Users Manual*, Department of Homeland Security, Emergency Preparedness Response Directorate, Washington, D.C.

Federal Emergency Management Agency (FEMA), 2000a. *FEMA 350 - Recommended Seismic Design Criteria for New Steel Moment-Frame Buildings*, Federal Emergency Management Agency, Washington, D.C.

Federal Emergency Management Agency (FEMA), 2000b. *FEMA 356 - Prestandard Commentary for the Seismic Rehabilitation of Buildings*, Federal Emergency Management Agency, Washington DC.

Federal Emergency Management Agency (FEMA), 2000c. *FEMA - 349: Action Plan for Performance-Based Seismic Design*, Federal Emergency Management Agency, Washington, D.C.

Federal Emergency Management Agency (FEMA), 2000d. *State of the Art Report on Performance Prediction and Evaluation of Steel Moment Frame Buildings, FEMA 355F*, Federal Emergency Management Agency, Washington, D.C.

Federal Emergency Management Agency (FEMA), 2000e. *State of the Art Report on Systems Performance of Steel Moment Frames Subjected to Earthquake Ground Shaking, FEMA 355C*, Federal Emergency Management Agency, Washington, D.C.

Federal Emergency Management Agency (FEMA), 2006. *FEMA 445: Next-Generation Performance-Based Seismic Design Guidelines*, Federal Emergency Management Agency, Washington, D.C.

Federal Emergency Management Agency (FEMA), 2007. *FEMA 461: Interim Testing Protocols for Determining the Seismic Performance Characteristics of Structural and Nonstructural Components*, Federal Emergency Management Agency, Washington, D.C.

Federal Emergency Management Agency (FEMA), 2008. *FEMA P695: Quantification of Building Seismic Performance Factors*, ATC-63 Project (90% Draft), Federal Emergency Management Agency, Washington, D.C.

Foley, C. M. 2007. Structural optimization using evolutionary computation, in *Optimization of Structural and Mechanical Systems*, J. S. Arora, ed., *World Scientific*, 59–120.

Foley, C. M., Pezeshk, S., and Alimoradi, A. 2007. Probabilistic performance-based optimal design of steel moment resisting frames: Part I – Formulation, *Journal of Structural Engineering* **133**, 757–766.

Foley, C. M., and Schinler, D. 2001. Optimized Design of Steel Frames Using Distributed Plasticity. 2001 Structures Congress, Washington, D.C., American Society of Civil Engineers, CD-ROM.

Foley, C. M., and Schinler, D. 2003. Automated Design of Steel Frames Using Advanced Analysis and Object-Oriented Evolutionary Computation. Journal of Structural Engineering, 129(5), American Society of Civil Engineers, 648–660.

Foley, C. M., Schinler, D., and Voss, M. S. 2002. Optimized Design of Fully and Partially Restrained Steel Frames Using Advanced Analysis and Object-Oriented Evolutionary Computation. Technical Report Submitted to the National Science Foundation, Award Number CMS-9813216.

Goldberg, D. E. 1989. Genetic Algorithms in Search, Optimization, and Machine Learning, Addison-Wesley, Boston, MA.

Hamburger, R., Rojahn, C., Meohle, J., Bachman, R., Comartin, C., and Whittaker, A. 2004 The ATC-58 Project: Development of Next-Generation Performance-Based Earthquake Design Criteria for Buildings. 13th World Conference on Earthquake Engineering, Vancouver, BC, Canada, CD-ROM.

Hamburger, R. H. 2004 Development of Next-Generation Performance-Based Earthquake Engineering Design Criteria for Buildings. Proceedings of the 13th World Conference on Earthquake Engineering (WCEE), Vancouver, BC, Canada, (CD-ROM).

Krawinker, H. 2006 Performance Assessment of an Old RC Frame Building - A PEER Testbed Study. 8th U.S. National Conference on Earthquake Engineering, San Francisco, CA, Earthquake Engineering Research Institute, CD-ROM.

Liu, M., Burns, S. A., and Wen, Y. K. 2003. Optimal Seismic Design of Steel Frame Buildings Based on Life-Cycle Cost Considerations. Earthquake Engineering and Structural Dynamics, 32, John Wiley & Sons, 1313–1332.

Liu, M., Burns, S. A., and Wen, Y. K. 2004a. Life-Cycle Cost Oriented Seismic Design Optimization of Steel Moment Frame Structures with Risk-Taking Preference. Engineering Structures, 26, Elsevier, Ltd., UK, 1407–1421.

Liu, M., Burns, S. A., and Wen, Y. K. 2004b Multiobjective Optimization for Performance-Based Seismic Design of Steel Moment Frame Structures. Proceedings of the 2004 Structures Congress, Nashville, TN, American Society of Civil Engineers, Reston, VA, CD-ROM.

Liu, M., Burns, S. A., and Wen, Y. K. 2005. Multiobjective Optimization for Performance-Based Seismic Design of Steel Moment-Frame Structures. Earthquake Engineering and Structural Dynamics, 34, John Wiley & Sons, 289–306.

Liu, M., Burns, S. A., and Wen, Y. K. 2006. Genetic Algorithm Based Construction-Conscious Minimum Weight Design of Seismic Moment-Resisting Frames. Journal of Structural Engineering, 10(4), American Society of Civil Engineers, Reston, VA, 468–481.

Miranda, E., and Aslani, H. 2003. Probabilistic Response Assessment for Building Specific Loss Estimation. PEER 2003/03, Pacific Earthquake Engineering Research Center.

Moehle, J., and Deierlein, G. 2004 A Framework Methodology for Performance-Based Earthquake Engineering. 13th World Conference on Earthquake Engineering, Vancouver, BC, Canada, CD-ROM.

Powell, G. H. 1993. DRAIN-2-DX Element Description and Users Guide for Element Type 01, Type 02, Type 04, Type 06, Type 09, Type 15, Version 1.10. Report No. UCB/SEMM-93/17-18, University of California - Berkeley, Berkeley, CA.

Prakash, V., Powell, G. H., and Campbell, S. 1993. DRAIN-2-DX Base Program Description and User Guide, Version 1.10. Report No. UCB/SEMM-93/17-18, University of California - Berkeley, Berkeley, CA.

Risk Engineering Inc. 2005. EZ-FRISK Version 7.14, User's Manual. Risk Engineering Inc., Software for Earthquake Ground Motion Estimation.

Rojas, H. 2008. Automating the Design of Steel Moment-Frames Using a Probabilistic-Based Approach and Evolutionary Computation, PhD Thesis, The University of Memphis.

Rojas, H., Pezeshk, S., and Foley, C. M. 2007. Performance-Based Optimization Considering Both Structural and Nonstructural Components. Earthquake Spectra, 23(3), Earthquake Engineering Research Institute, 685–709.

Schinler, D., and Foley, C. M. 2001 An Object-Oriented Evolutionary Algorithm for Advanced Analysis-Based Design. Genetic and Evolutionary Computation Conference (GECCO) Workshop, San Francisco, CA, Morgan Kaufmann, 73–78.

Somerville, P., Smith, N. F., Punyamurthula, S., and Sun, J. 1997. Development of Ground Motion Time Histories for Phase 2 of the FEMA/SAC Steel Project (Report No. SAC/BD-97-04), SAC Joint Venture, Sacramento, CA.

Tsompanakis, Y., and Papadrakakis, M. 2006. Large-Scale Reliability-Based Structural Optimization. Structural and Multidisciplinary Optimization, Springer, Berlin/Heidelberg, (on-line first).

Voss, M. S., and Foley, C. M. 1999a Evolutionary Algorithm for Structural Optimization. Proceedings of the Genetic and Evolutionary Computation Conference (GECCO), Orlando, FL, Morgan Kaufman, 678–685.

Voss, M. S., and Foley, C. M. 1999b The (mu, lambda, alpha, beta) Distribution: A Selection Scheme for Ranked Populations. Proceedings of the Genetic and Evolutionary Computation Conference (GECCO) - Late Breaking Papers, Orlando, FL, Morgan Kaufman, 284–291.

Zareian, F., and Krawinker, H. 2006a Simplified Performance-Based Earthquake Engineering. 8th U.S. National Conference on Earthquake Engineering, San Francisco, CA, Earthquake Engineering Research Institute, CD-ROM.

Zareian, F., and Krawinker, H. 2006b Why and How to Predict the Probability of Collapse of Buildings. 8th U.S. National Conference on Earthquake Engineering, San Francisco, CA, Earthquake Engineering Research Institute, CD-ROM.

(Received 21 April 2009; accepted 27 August 2010)